Effects of Hydroxyl Groups and Architecture of Organic Polymers on Polystyrene/Silica Nanocomposites

Reiko Saito, Shin-ichiro Kobayashi, Takayoshi Hosoya

Department of Organic and Polymeric Materials, Tokyo Institute of Technology, 2–12-1-S1–22, Ookayama, Meguro-ku, Tokyo, 152-8552, Japan

Received 12 April 2004; accepted 19 November 2004
DOI 10.1002/app.21959
Published online in Wiley InterScience (www.interscience.wiley.com).

ABSTRACT: Transparent polystyrene/silica nanocomposites were synthesized by casting the blend solutions of polystyrene (PS) derivatives and perhydropolysilazane (PHPS) and by calcinating the blend films of PS derivatives and PHPS at 100°C for 3 h under steam. Poly(styrene-*co*-4-vinyl phenol)s [P(S-*co*-VPh)s], poly(styrene-*co*-hydroxymethyl styrene)s [P(S-*co*-HMS)s], poly(styrene-*co*-4-vinyl phenol)-*block*-PSs [P(S-*co*-VPh)-*block*-PSs], and poly(styrene-*co*-hydroxymethyl styrene)-*block*-PSs [P(S-*co*-HMS)-*block*-PSs] were used as the PS derivatives. The morphology of the microphase separation, transparency, the degree of grafting of PHPS onto PS derivatives, and surface hardness of the composites were investigated by transmission electron microscopy, UV–vis, FTIR, and nanoindentation, respectively. Degrees of grafting of PHPS onto PS derivatives and transparency of the composites of P(S-*co*-VPh)s and P(S-*co*-VPh)-*block*-PSs were higher than those of P(S-*co*-HMS)s and P(S-*co*-HMS)-*block*-PSs. Surface hardness of the composites of P(S-*co*-VPh)-*block*-PS was drastically increased from 0.22 to 0.55 GPa by increasing the weight fraction of silica to 33.7%.
 J Appl Polym Sci 97: 1835–1847, 2005

Key words: silicas; polystyrene; nanocomposites; coating; hardness

INTRODUCTION

Silica has been blended with organic polymers to improve the properties of organic polymers. For example, transparency, mechanical strength, and thermal stability of poly(meth)acrylates were greatly improved by the blending of silica.[1–6] On the other hand, the transparent PS/silica composite was rarely obtained due to the macroscopic phase separation of silica and PS in a few micrometers owing to the incompatibility of PS and silica. Thus, it is difficult to synthesize transparent PS/silica composites in a wide range of silica content. To reduce the macroscopic phase separation of PS and silica in the composites, several interesting approaches have been investigated. Hsiue and colleagues prepared highly transparent PS/silica nanocomposites by a sol-gel method from copolymer of styrene and an alkoxysilane-containing monomer, methacrylic acid 3-(trimethoxysilyl)propyl ester (MAMSE).[7] The sol-gel method is one of the most convenient methods to synthesize organic/silica composites at low temperature.[8,9] However, silica synthesized by the sol-gel method contains many lattice defects. The sol-gel method also requires catalysts that may be impurities in the composites.

Silica is also synthesized from perhydropolysilazane (PHPS; Fig. 1) with mild conditions without a specific catalyst except for steam. The densities and refractive index of silica prepared from PHPS are very close to silica glass. Since PHPS is soluble to many organic solvents, such as benzene, xylene, tetrahydrofurane (THF), pyridine, and so forth, organic solutions of PHPS are used for silica coatings. However, the reported maximum thickness of silica coat film by using PHPS solutions was less than 2.2 μm due to the drastic shrinkage of coat film owing to the density change from 1.3 to 2.2 g/cm^3 by calcination.

Another interesting feature of PHPS is its high reactivity with the hydroxyl group. PHPS can be grafted onto organic polymers composing hydroxyl groups in organic solvents. It is well known that block and graft copolymers with incompatible sequences form microphase separation in the solid state.[10,11] When PHPS and organic polymers composing hydroxyl groups are blended in organic solvents, graft copolymer with organic truck and PHPS branches is formed in solution. The organic/PHPS composite with microphase separated domains of the organic polymer and PHPS is obtained by casting of the blend solution of PHPS and the organic polymer. When the calcination temperature of PHPS is lower than the glass transition temperature, Tg, of the organic polymer, the morphology of microphase separation of the composite is not changed by calcination. The calcination temperature of PHPS, 100°C, is lower than the Tg of many organic polymers. Therefore, an organic/silica nanocomposite with controlled morphology is obtained (Fig. 2).

Correspondence to: R. Saito (rsaito@polymer.titech.ac.jp).

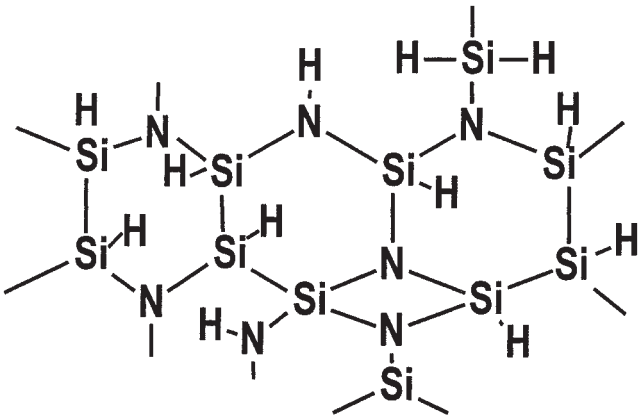

Figure 1 Structure of perhydropolysilazane (PHPS).

Based on this concept, poly(methyl methacrylate) (PMMA)/silica nanocomposites were synthesized with poly(methyl methacrylate-*co*-2-hydroxyethyl methacrylate) (P(MMA-*co*-HEMA))[12] and PMMA-*block*-P(MMA-*co*-HEMA).[13,14] The morphology of the nanocomposites was well-controlled with PMMA-*block*-P(MMA-*co*-HEMA) rather than P(MMA-*co*-HEMA)[13] due to the strong segregation of PMMA of PMMA-*block*-P(MMA-*co*-HEMA) rather than P(MMA-*co*-HEMA). Well-defined PMMA/silica nanocomposites with PMMA and silica lamellae were successfully synthesized by soaking of microphase separated films of PMMA and PHEMA lamellae composites with PMMA-*block*-PHEMA in the PHPS solutions.[15] The thermal decomposition behaviors of the organic domains of the composites were not similar to PMMA-*block*-PHEMA but PMMA due to the complete phase separation of PMMA and silica in the nanocomposites.

This method is applicable to base polymers, such as poly(2-vinyl pyridine) (P2VP), poly(4-vinyl pyridine) (P4VP),[16,17] and so forth. Generally, the basic polymers react with the catalyst of the sol-gel method. However, they don't react with PHPS; the P2VP/silica and P4VP/silica nanocomposites were obtained by blending of PHPS to P(2VP-*co*-HEMA) and P(4VP-*co*-HEMA), respectively. The values of leakage current of the P2VP-PMMA/silica nanocomposites were drastically decreased from P(2VP-*co*-MMA) in spite of the fact that refractive indexes, dielectric constants, and field break down values were not changed.[16]

As well as the PMMA/silica, P2VP/silica, P4VP/silica nanocomposites, and PS/silica nanocomposites will be synthesized with PHPS and PS derivatives containing hydroxyl groups. If HEMA is a comonomer of the PS derivatives as a reaction site with PHPS, the strong segregation between PS and HEMA causes the formation of aggregates of organic polymers, such as micelles. Then, well-arranged morphology of the nanocomposites will not be obtained. Additionally, it was already found that the high reactivity of HEMA cased the gelation of the blend solution of organic polymer and PHPS because each PHPS molecule has multi-reactive sites. If the reactivity of hydroxyl groups with PHPS is reduced and the compatibility between styrene and comonomer containing hydroxyl groups is increased, transparent PS/silica nanocomposites with better control of morphology of the microphase separation are expected. The purpose of this

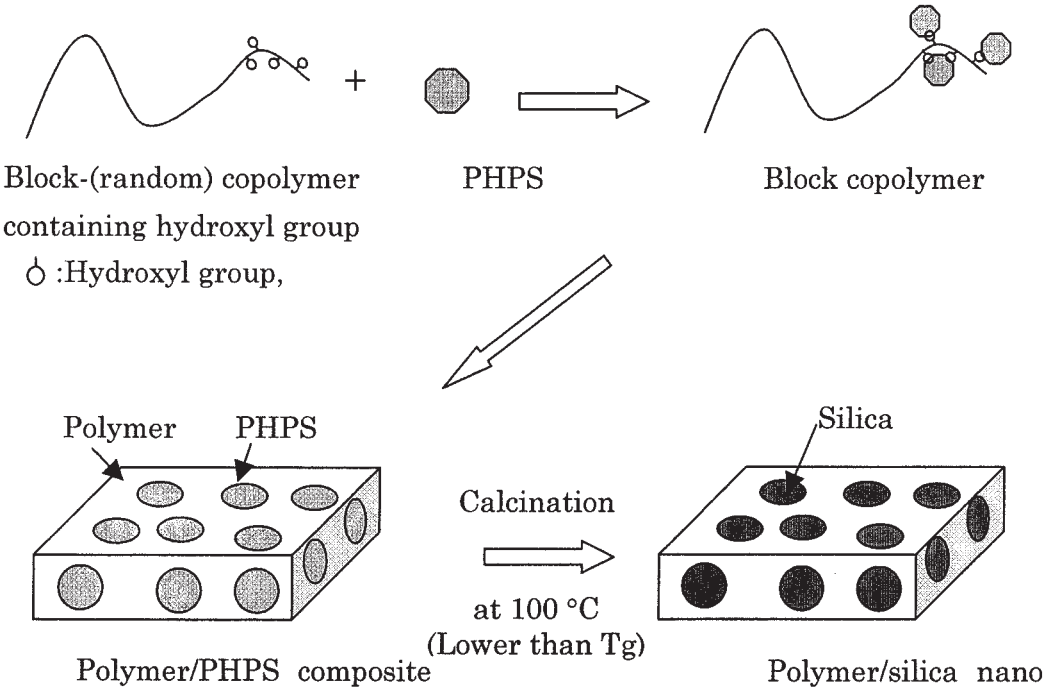

Figure 2 Synthesis of organic/silica nanocomposites with perhydropolysilazane (PHPS).

study is to synthesize transparent PS/silica nanocomposites by blending of PS derivatives and PHPS.

As described above, the reduction of reactivity of hydroxyl groups with PHPS is important. Thus, 4-vinyl phenol (VPh) and *p*-hydroxymethyl styrene (HMS) were chosen as comonomers containing phenolic and alcoholic hydroxyl groups, respectively. The architectural effect on the control of morphology of microphase separation of PS/silica nanocomposites was investigated by using the block copolymers P(S-*co*-VPh)-*block*-PS and P(S-*co*-HMS)-*block*-PS, and the random copolymers P(S-*co*-VPh) and P(S-*co*-HMS). The morphology of microphase separation of the nanocomposites was investigated by transmission electron microscopy (TEM).

One of the most interesting features of this method is that the nanocomposite is formed by casting the blend solution of PHPS and the organic polymers. This technique will be applied to coating technique. Generally, the silica coat provides a hard surface.[18–22] Thus, the microscopic hardness of the nanocomposite formed on the glass surface and their self-standing composites was quantitatively investigated by a nanoindentation technique.

EXPERIMENTAL

Materials

Styrene (S: Kanto, 99%), *tert*-butoxyl-*p*-styrene (BS, Wako pure chemicals, 98%), and 4-chloromethyl styrene (CMS, Aldrich 95%) were purified by distillation under vacuum. Other reagents were used as received.

Synthesis of poly(styrene-*co*-*tert*-butoxy-*p*-styrene) [P(S-*co*-BS)] and poly(styrene-*co*-4-chloromethyl styrene) [P(S-*co*-CMS)]

Predetermined amounts of monomers, α, α'-azobis isobutylonitril (AIBN, Kanto, 97%) as an initiator, and benzene (Kanto, 99.5%) were sealed in glass ampoules *in vacuo*. The sealed ampoules were heated at 60°C for 45 h. After the reaction, the polymer was precipitated in methanol (Kanto, 99.8%) and purified with benzene and methanol by the re-precipitation method. Polymerization conditions are listed in Table I. Purified polymer was freeze-dried, and characterized by ^{1}H NMR and GPC.

Synthesis of poly(styrene-*co*-*tert*-butoxy-*p*-styrene) macroinitiator [P(S-*co*-BS)-TEMPO] and poly(styrene-*co*-4-chloromethyl styrene) macroinitiator [P(S-*co*-CMS)-TEMPO]

Predetermined amounts of 4-methoxy-2,2,6,6,-tetranethylpiperidine-1-oxyl (4-MTEMPO, Tokyo Chemical Industry, 98%) and benzoyl peroxide (BPO, Nakarai Techs, 75%) were added to a mixture of S and BS or CMS in a glass ampoule. The glass ampoules were sealed *in vacuo* and heated at 80°C for 6 h. After heating, the ampoules were cooled at −78°C with a dry ice/methanol mixture, and a predetermined amount of acetic acid anhydride (Kanto, 97%) was added to the ampoule. Then, the ampoule was sealed under vacuum and heated at 125°C for 4.5–9.0h. Polymerization conditions are listed in Table I. After the polymerization, the products, that is, the macroinitiators, were precipitated with methanol, purified with benzene and methanol by the reprecipitation method, and characterized by GPC and ^{1}H NMR. When the molecular weight distribution, M_w/M_n, of the macroinitiator was larger than 1.4, the macroinitiator was fractionated with benzene and methanol.

Synthesis of poly(styrene-*co*-*tert*-butyoxy-*p*-styrene)-*block*-polystyrene [P(S-*co*-BS)-*block*-PS] and poly(styrene-*co*-4-chloromethyl styrene)-*block*-polystyrene [P(S-*co*-CMS)-*block*-PS]

Predetermined amounts of P(S-*co*-BS)-TEMPO macroinitiator or P(S-*co*-CMS)-TEMPO macroinitiator were dissolved in a mixture of predetermined amounts of S and 4-MTEMPO in a glass ampoule. After dissolution, a certain amount of acetic acid anhydride was added to the glass ampoule. The ampoule was sealed under vacuum, and heated at 125°C for 7–20.5 h. Polymerization conditions are listed in Table I. After polymerization, the polymer was precipitated with methanol, purified with benzene and methanol by the reprecipitation method, freeze-dried, and characterized by ^{1}H NMR and GPC. When M_W/M_n was larger than 1.4, the polymer was fractionated with methanol and benzene.

Synthesis of poly(styrene-*cop*-hydroxymethyl styrene) [P(S-*co*-HMS)] and poly(styrene-*cop*-hydroxymethyl styrene)-*block*-polystyrene [P(S-*co*-HMS)-*block*-PS] by hydrolysis of P(S-*co*-CMS) and P(S-*co*-CMS)-*block*-PS, respectively

A predetermined amount of P(S-*co*-CMS) or P(S-*co*-CMS)-*block*-PS was dissolved in benzene (polymer concentration 5 wt %), and 5 wt % of methanol to benzene and lithium hydroxide (Kanto, 90%) were added to the mixture. The mixture was refluxed at 60°C for 24 h. After the reaction, a small amount of water was added to the mixture and continuously stirred for 5 min. Then, the polymer was precipitated with *n*-hexane (Kanto, 96%), purified with benzene and *n*-hexane by the reprecipitation method, freeze-dried with benzene, and characterized by Volhart's titration as described later. Conditions and results are listed in Table II.

Synthesis of poly(styrene-*co*-4-vinyl phenol) [P(S-*co*-VPh)] and poly(styrene-*co*-4-vinyl phenol)-*block*-polystyrene [P(S-*co*-VPh)-*block*-PS] by hydrolysis of P(S-*co*-BS) and P(S-*co*-BS)-*block*-PS, respectively

Hydrolysis of butoxy styrene was carried out as follows: A predetermined amount of P(S-*co*-BS) or P(S-

TABLE I
Conditions and Results of Synthesis of P(S-*co*-CMS)s, P(S-*co*-BS)s, and P(S-*co*-CMS)-TEMPO Macroinitiators, P(S-*co*-BS)-TEMPO Macroinitiators, PS-*block*-P(S-*co*-CMS)s, and PS-*block*-P(S-*co*-BS)s

Sample code	Initiator	Monomer			[Initiator]:[4 MTEMPO]:[Monomer]	Temp.[a] (°C)	Time[a] (h)	Yield (wt %)	Mn_{GPC}[b]	Mw/Mn[b]	BS or CS content[c] (mol%)	Formula[d]
		S (mol)	BS (mol)	CS (mol)								
RSC1	AIBN	0.1731	0	0.0122	1:0:160	60	50	55.4	2.40×10^4	1.49	6.5	$P(S_{209}\text{-}co\text{-}CMS_{15})$
RSC2	AIBN	0.1731	0	0.0245	1:0:178	60	50	63.1	2.40×10^4	1.46	14.2	$P(S_{186}\text{-}co\text{-}CMS_{31})$
RSC3	AIBN	0.1731	0	0.0368	1:0:251	60	50	57.3	2.60×10^4	1.63	25.0	$P(S_{168}\text{-}co\text{-}CMS_{56})$
RSB1	AIBN	0.1731	0.0071	0	1:0:317	60	50	48.8	3.00×10^4	1.51	7.3	$P(S_{255}\text{-}co\text{-}BS_{25})$
RSB2	AIBN	0.1731	0.0133	0	1:0:339	60	50	43.3	3.10×10^4	1.41	11.3	$P(S_{245}\text{-}co\text{-}BS_{31})$
RSB3	AIBN	0.1731	0.0269	0	1:0:363	60	50	38.3	2.80×10^4	1.43	18.8	$P(S_{193}\text{-}co\text{-}BS_{45})$
SC1	BPO	0.0106	0	0.0026	1:1.22:70	80/125	6/9	50.5	1.97×10^4	1.17	25.0	$P(S_{127}\text{-}co\text{-}CMS_{42})$-TEMPO
SC2	BPO	0.0086	0	0.0042	1:1.20:70	80/125	7.0/6.0	66.2	3.78×10^4	1.16	39.8	$P(S_{185}\text{-}co\text{-}CMS_{122})$-TEMPO
SC3	BPO	0	0	0.0110	1:1.21:69	80/125	5.5/6.0	55.7	2.24×10^4	1.23	100.0	$PCMS_{147}$-TEMPO
SB1	BPO	0.0986	0.0250	0	1:1.25:71	80/125	6.0/5.0	56.7	2.19×10^4	1.2	27.3	$P(S_{129}\text{-}co\text{-}BS_{48})$-TEMPO
SB2	BPO	0.0768	0.0382	0	1:1.24:71	80/125	6.0/5	50.8	2.24×10^4	1.23	41.7	$P(S_{97}\text{-}co\text{-}BS_{70})$-TEMPO
SB3	BPO	0	0.0850	0	1:1.20:60	80/125	6.5/5	65.6	5.74×10^4	1.41	100.0	PBS_{326}-TEMPO
BSC1	SC1	0.2010	0	0	1:3.26:1970	125	10	26.1	1.00×10^5	1.32	2.3	$P(S_{127}\text{-}co\text{-}CMS_{22})\text{-}block\text{-}PS_{782}$
BSC2	SC2	0.1570	0	0	1:1.00:3950	125	7.2	31.4	1.34×10^5	1.44	4.1	$P(S_{185}\text{-}co\text{-}CMS_{52})\text{-}block\text{-}PS_{958}$
BSC3	SC3	0.2010	0	0	1:3.37:2250	125	10	22.4	1.36×10^5	1.43	4.4	$PCMS_{56}\text{-}block\text{-}PS_{1135}$
BSB1	SB1	0.1480	0	0	1:2.74:2160	125	10	27.5	9.67×10^4	1.32	5.8	$P(S_{129}\text{-}co\text{-}BS_{52})\text{-}block\text{-}PS_{717}$
BSB2	SB2	0.1830	0	0	1:1.05:6160	125	10	29.5	1.08×10^5	1.28	6.1	$P(S_{97}\text{-}co\text{-}BS_{61})\text{-}block\text{-}PS_{829}$
BSB3	SB3	0.1480	0	0	1:3.07:4240	125	8	23.3	1.45×10^5	1.4	13.6	$PBS_{173}\text{-}block\text{-}PS_{948}$

Acetic acid anhydride: 1 wt % to a polymerization mixture. Solvent: Benzene with [M_0]: 5 wt % for RSC1–3 and RSB1–3. Bulk for SC1–3, SB1–3, BSC1–3, and BSB1–3.

[a] Before addition of acetic anhydride/after addition of acetic anhydride.

[b] Determined by GPC calibrated with PS standards.

[c] Determined by ^1H NMR.

[d] S, CMS, and BS indicate styrene, chloromethyl styrene, and *tert*-butoxy styrene. Number after the name of the monomer indicates the degree of polymerization of the monomer.

TABLE II
Conditions and Results of Hydrolysis with Chloromethyl Styrene Unit

Code	Precursor polymer	Degree of hydrolysis (%)	OH content[a] (mol %) In random sequence	OH content[a] (mol %) In whole polymer	Formula[b]
RSH1	RSC1	47.7	3.1	3.1	$P(S_{209}\text{-}co\text{-}CMS_{8}\text{-}co\text{-}HMH_{7})$
RSH2	RSC2	43.4	6.2	6.2	$P(S_{186}\text{-}co\text{-}CMS_{18}\text{-}co\text{-}HMS_{13})$
RSH3	RSC3	55	13.8	13.8	$P(S_{168}\text{-}co\text{-}CMS_{25}\text{-}co\text{-}HMS_{31})$
BSH1	BSC1	64.5	16.1	1.48	$P(S_{127}\text{-}co\text{-}CMS_{14}\text{-}co\text{-}HMS_{8})\text{-}block\text{-}PS_{782}$
BSH2	BSC2	72	28.7	2.95	$P(S_{185}\text{-}co\text{-}CMS_{15}\text{-}co\text{-}HMS_{37})\text{-}block\text{-}S_{958}$
BSH3	BSC3	62.5	62.5	2.75	$P(CMS_{21}\text{-}co\text{-}HMS_{35})\text{-}block\text{-}PS_{1135}$

[a] Determined by ^{1}H NMR.
[b] S, CMS, and HMS indicate styrene, chloromethyl styrene, and hydroxymethyl styrene. Number after monomer name indicates the degree of polymerization of the monomer unit.
Polymer concentration: 3.7 wt %. Solvent: benzene/methanol (5/1 v/v). [LiOH]/[CMS] = 1.5. Temperature: 60°C, time: 24–36h.

co-BS)-*block*-PS was dissolved in a benzene (Kanto) and THF (Kanto) mixture with 5 wt % of THF. Polymer concentration was set to 5 wt %. 2,2,2-Trifluoroethanol (Aldrich, 99%) and trifluoromethanesulfonic acid (Aldrich, 98%) were added to the mixture at 0°C. The mixture was stirred at 0°C for 20 min. After the reaction, a small amount of water was added to the mixture and continuously stirred for 5 min. Then, the polymer was precipitated with *n*-hexane, purified with benzene and *n*-hexane by the reprecipitation method, freeze-dried with benzene, and characterized by the UV method described later. The conditions and results are listed in Table III.

Preparation of the composites

Polymers were dissolved in THF (Kanto, 99.5%) with 1 wt % of polymer concentration. Then, perhydropolysilazane (PHPS)-xylene solution (NN-110, Clariant Japan, Co., average molecular weight of PHPS: 700) was added to the polymer solution under a dry nitrogen atmosphere. The reaction was carried out at ambient temperature for 24 h under nitrogen. After the reaction, the solution was cast on a Teflon dish and flat glass and gradually dried under nitrogen, to form self-standing film and coat film on the glass, respectively. For the measurement of degree of grafting, a small amount of the solution was sampled before casting. Polymer in the sampled solution was precipitated with *n*-hexane, dried, and characterized with an FTIR spectroscope (Jasco, FT/IR-410).

The self-standing film and the coat film were exposed to vapor of a triethylamine-water solution (triethyl amine (Tokyo Chemical Industry, 99%) concentration: 5 wt %) for 3 min, and continuously heated at 100°C for 3 h under steam. Composites were characterized by FT-IR, UV–vis, transmission electron microscopy (TEM), differential scanning calorimetry (DSC), and surface hardness measurements.

Measurement

Number average molecular weight, M_n, and M_w/M_n were measured with gel-permeation chromatography (Tosoh, HPLC-8020) with a guard column and a 30-cm mixed column (Tosoh $TSK_{gel}G\text{-}5000H_{HR}$) with a dif-

TABLE III
Conditions and Results of Hydrolysis of Butoxy Styrene Unit

Code	Precursor polymer	Degree of hydrolysis (%)	OH content[a] (mol %) In random sequence	OH content[a] (mol %) In whole polymer	Formula[b]
RSPh1	RSB1	47.7	3.5	3.5	$P(S_{255}\text{-}co\text{-}BS_{13}\text{-}co\text{-}VPh_{12})$
RSPh2	RSB2	58.1	6.6	6.6	$P(S_{245}\text{-}co\text{-}BS_{13}\text{-}co\text{-}VPh_{18})$
RSPh3	RSB3	53.8	10.1	10.1	$P(S_{193}\text{-}co\text{-}BS_{21}\text{-}co\text{-}VPh_{24})$
BSPh1	BSB1	100	27.3	5.7	$P(S_{129}\text{-}co\text{-}VPh_{52})\text{-}block\text{-}PS_{717}$
BSPh2	BSB2	100	41.7	6.1	$P(S_{97}\text{-}co\text{-}VPh_{61})\text{-}block\text{-}PS_{829}$
BSPh3	BSB3	100	100	13.6	$P(VPh_{173})\text{-}block\text{-}PS_{948}$

[a] Determined by ^{1}H NMR.
[b] S, BS, and VPh indicate styrene, butoxystyrene, and 4-vinyl phenol. Number after monomer name indicates the degree of polymerization of the monomer unit.
Polymer concentration: 2.0 wt %. Solvent: benzene/THF (20/1 v/v). [BS]:[CF_3CH_2OH]:[CF_3SO_3H] = 1:5:1.
Temperature: 0°C, time: 20 min.

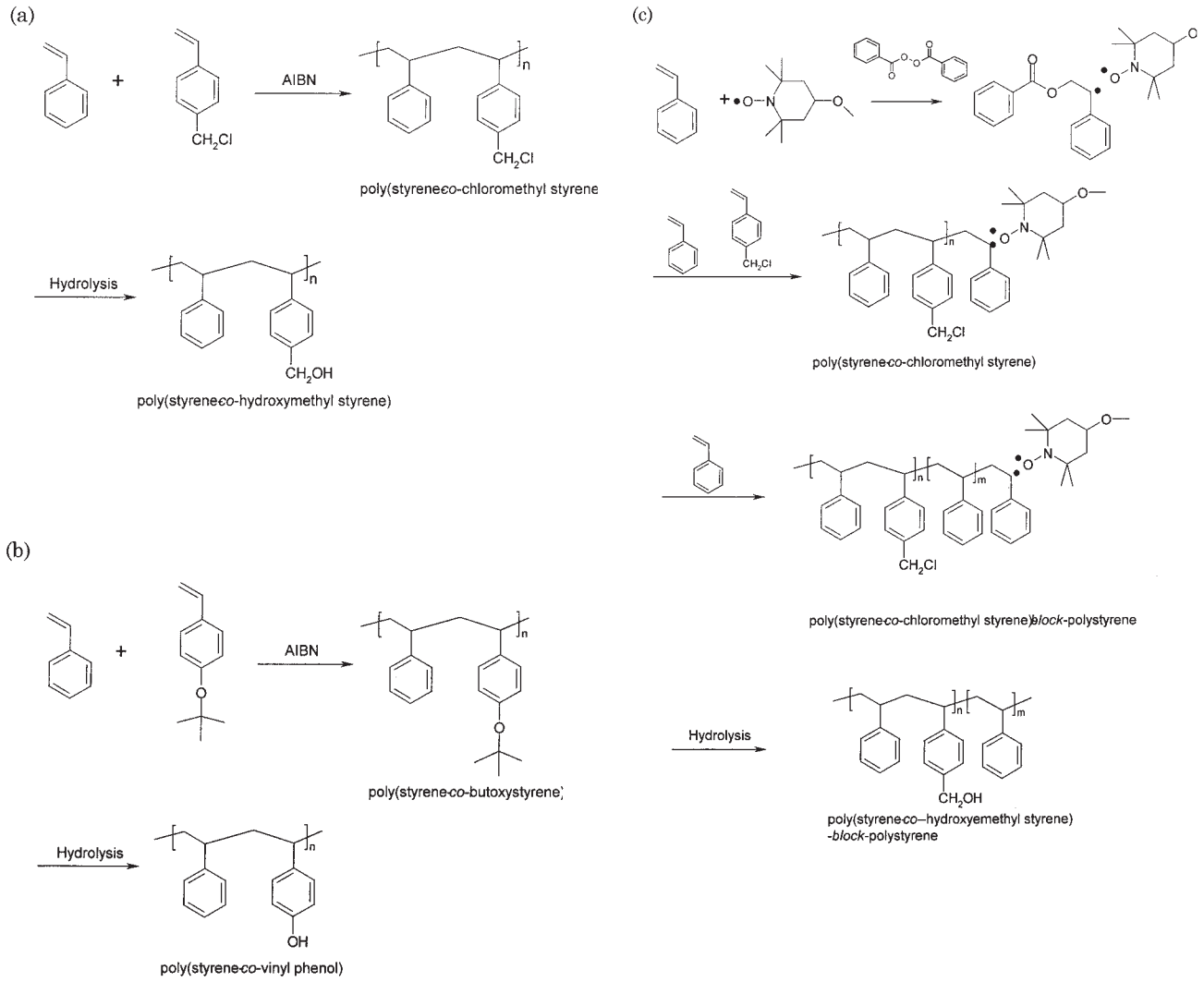

Figure 3 Synthesis of polymers: (a) P(S-*co*-HMS), (b) P(S-*co*-VPh), (c) P(S-*co*-HMS)- *block*-PS, and (d) P(S-*co*-VPh)-*block*-PS.

ferential refractive index detector (Tosoh, RI-8020) with THF at 0.6 mL min^{-1} as an eluent at 35°C. PS standards (Tosoh) in the range 4.0×10^3 to 3.18×10^5 g mol^{-1} were used to calibrate the GPC.

^1H NMR spectra were recorded at 500 MHz on a JEOL GLX-500 spectrometer with *d*-chloroform (Aldrich, 99.9%) as a solvent.

FTIR spectra of P(S-*co*-BS)-*block*-PS and P(S-*co*-VPh)-*block*-PS were measured with an FTIR spectrometer (Jasco, FT/IR-410) by the KBr method. Degree of hydrolysis was estimated by using the peaks at 3200–3700 and 1364 cm^{-1} owing to hydroxyl and *tert*-butoxy groups, respectively.

For the UV measurements of P(S-*co*-BS) and P(S-*co*-VPh), polymers were dissolved in THF (polymer concentration: 5 wt %). Then, 10 wt % of pyridine (Kanto, 99.7%) to benzene and 2-naphthoyl chloride (Aldrich, 98%) were added to the mixture. The mixture was stirred at room temperature overnight. After the reaction, the polymer was precipitated with methanol, purified with THF and methanol, and freeze-dried. The degree of hydrolysis was calculated from the absorbance of UV measurements of dried polymer-THF mixtures, carried out with a UV-VIS spectrometer (Jasco, V-530) at 338 nm.

Dynamic light scattering (DLS) measurements of the polymer solutions were carried out at 90 degrees at room temperature with a DLS spectrometer (Photal, ELS-8000).

For Volhart's titration, 0.1 g P(S-*co*-HMS) and P(S-*co*-HMS)-*block*-PS were dissolved in 10 mL THF in glass ampoules, then excess amounts of solidum metal (Kanto) and naphthalene (Kanto) were added. The ampoules were sealed and stirred at room temperature until the solution became dark green. After the reaction, sodium remaining in the solution was removed; and 10 mL methanol, 30 mL benzene, 30 mL water, and 0.2 mL of concentrated hydro nitride (Kanto, d = 1.42) were added to the solution. The solution was stirred at ambient temperature overnight. A certain amount of silver nitride aqueous was added and stirred overnight. Then the Volhart's titration was carried out with NH_4SCN.

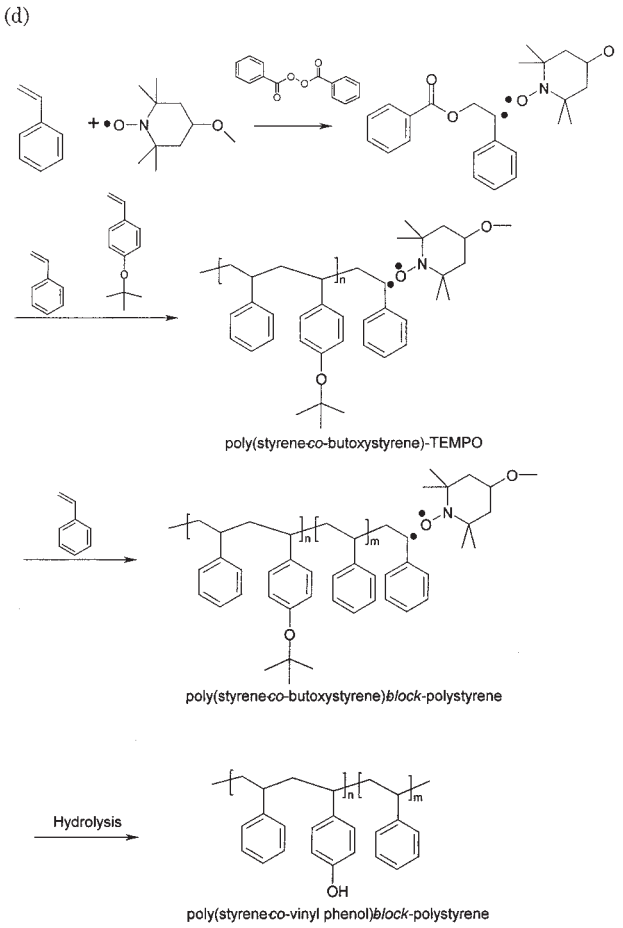

Figure 3 (*Continued from the previous page*)

The degrees of hydrolysis of P(S-*co*-HMS) and P(S-*co*-HMS)-*block*-PS were calculated from the remaining amount of CMS in polymers.

A TEM specimen was prepared by casing the sampled solution on copper microgrids coated with carbon substrate and the calcination, and observed with a transmission electron microscope (JEOL, TEM200-CX, 100 kV). For polymers, the specimens were stained with OsO_4 gas.

DSC measurements were carried out for 4 mg of samples sealed in aluminum pans with a differential scanning calorimeter (Perkin–Elmer, Pyris) in the range from 50 to 250°C with temperature increasing at 10°C min^{-1}.

Surface hardness of the self-standing films and the coat films were recorded with a nanoindentor (triboscope, Hysitron, Inc.) attached to an atomic force microscope (AFM, SPM9500J2, Shimazu). The hardness measurements were performed with a load ranging from 50 to 5000 μN, corresponding to a contact depth from 50 to 1200 nm.

RESULTS AND DISCUSSION

Synthesis of organic polymers

As described above, hydroxymethyl styrene (HMS) and vinyl phenol (VPh) were chosen as the hydroxyl groups. It is difficult to homogeneously copolymerize styrene and HMS or VPh because of their incompatibility with styrene (S). In contrast, chloromethyl styrene (CMS) and butoxy styrene (BS), which provide HMS and VPh, respectively, by hydrolysis, are compatible with S. Thus, P(S-*co*-CMS), P(S-*co*-BS), P(S-*co*-CMS)-*block*-PS, and P(S-*co*-BS)-*block*-PS were polymerized, then they were hydrolyzed (Fig. 3). For random copolymers, it is not necessary to control the molecular weight distribution. Thus, P(S-*co*-CMS)s [RSC series] and P(S-*co*-BS)s [RBS series] were synthesized by conventional radical polymerization with AIBN. Results of the polymerization are listed in Table I. The molecular weights of the RSC series and the RSB series are between $\sim 2.4 \times 10^4$ and 3.0×10^4, respectively. The molecular weight distributions of all random copolymers (1.41–1.63) were narrow. Content of CMS and BS were varied from 6.5 to 25 mol %. Random copolymers of the RSC series and the RSB series with relatively narrow molecular weight and various CMS and BS contents were obtained.

Block copolymers were also synthesized for more strict control of the microphase separation of the composites than random copolymers. Well-defined block copolymers were required for organic/silica nanocomposites with well-arranged structure. On the other hand, to avoid the gelation of the blend solution, the sequence with hydroxyl groups should be random copolymer of styrene and the monomer with the hydroxyl group. Thus, P(S-*co*-CMS)-*block*-PSs [BSC 1–3] and P(S-*co*-BS)-*block*-PSs [BSB 1–3] were synthesized by two step living radical polymerization with TEMPO. The results of the polymerization are listed in Table I. The molecular weights of the BSC series and the BSB series were close, in a range from 9.67×10^4 to 1.45×10^5, and the molecular weight distributions were relatively narrow (>1.44). The CMS or BS contents were varied from 2.3 to 13.6 mol % in the block copolymers. Thus, many types of block copolymers were obtained.

Then, all random and block copolymers were hydrolyzed to provide HMS and VPh units from CMS and BS units in the copolymers, respectively. The results are shown in Tables II and III. Except for the BSPh series in Table III, the hydrolysis was not completed. The maximum degree of hydrolysis was 72 mol % for BSH2 due to the drastic change of solubility of the copolymers in the solvent by hydrolysis. If the solvent for hydrolysis were changed, the degree of hydrolysis would be improved. However, the purpose of this section was not complete hydrolysis but the preparation of copolymers with different contents of hydroxyl groups. Therefore, further hydrolysis was not carried out. Random and block copolymers with different contents of hydroxyl group were obtained. After hydrolysis, the content of hydroxyl group in the copolymer was varied from 1.48 to 13.8 mol %. Here,

TABLE IV
Conditions and Results of Preparation of Composites

	Feed conditions						Results			
							Weight fraction of silica in composites (wt %)			
Code	Polymer type	NN-110/ Polymer (ml/g)	PHPS fraction in composite	[PHPS]/ [OH]	[PHPS]/ [OH] in copolymer	Reacted PHPS with polymer (mol %)	Whole in composite	Reacted silica with polymer	Unreacted silica with polymer	Solubility to THF
RSH1-0.6		0.62	10.22	0.60	0.41	69.16	8.83	6.10	2.72	o
RSH1-1.0	RSH1	1.16	17.65	1.00	0.36	35.56	15.41	5.48	9.93	o
RSH1-1.6		1.78	24.63	1.60	0.30	18.92	21.74	4.11	17.63	o
RSH2-0.5		1.10	16.82	0.50	0.24	47.16	14.67	6.92	7.75	o
RSH2-1.0	RSH2	2.19	28.73	1.00	0.26	26.37	25.52	6.73	18.79	o
RSH2-1.5		3.32	37.92	1.50	0.20	13.12	34.17	4.48	29.69	o
RSH3-0.5	RSH3	1.45	21.11	0.50	0.10	20.42	18.53	3.78	14.75	o
RSH3-1.0		4.90	47.42	1.00	0.10	9.57	43.39	4.15	39.23	o
RSH3-1.5	RSH3	7.37	57.55	1.50	0.10	6.59	53.54	3.53	50.01	o
RSPh1-0.7		0.85	13.54	0.70	0.88	100.00	11.75	11.75	0.00	x
RSPh1-1.1	RSPh1	1.33	19.69	1.10	0.98	88.99	17.24	15.34	1.90	x
RSPh1-1.3		1.68	23.62	1.30	1.12	86.23	20.81	17.95	2.87	x
RSPh2-0.7		1.64	23.14	0.70	0.71	100.00	20.37	20.37	0.00	x
RSPh2-1.0	RSPh2	2.43	30.93	1.00	0.80	80.45	27.57	22.18	5.39	x
RSPh2-1.4		3.25	37.43	1.40	0.85	60.68	33.70	20.45	13.25	x
RSPh3-0.8		2.74	33.49	0.80	0.53	66.34	29.97	19.88	10.09	x
RSPh3-1.1	RSPh3	4.02	42.53	1.10	0.82	74.14	38.61	28.63	9.99	x
RSPh3-1.5		5.39	49.81	1.50	1.12	74.72	45.76	34.19	11.57	x
BSH1-0.7		0.38	6.54	0.71	0.20	27.95	5.62	1.57	4.05	x
BSH1-1.1	BSH1	0.60	10.01	1.13	0.20	17.35	8.64	1.50	7.14	x
BSH1-1.6		0.83	13.26	1.55	0.15	9.68	11.50	1.11	10.39	x
BSH2-0.5	BSH2	0.56	9.37	0.53	0.36	68.55	8.08	5.54	2.54	x
BSH2-0.9		0.94	14.79	0.89	0.15	16.82	12.86	2.16	10.70	x
BSH2-1.4	BSH2	1.51	21.71	1.42	0.09	6.31	19.07	1.20	17.87	x
BSH3-0.7		0.71	11.56	0.72	0.53	72.82	10.00	7.28	2.72	x
BSH3-1.4	BSH3	1.33	19.68	1.35	0.40	29.93	17.24	5.16	12.08	x
BSH3-2.0		2.00	26.88	2.03	0.27	13.20	23.81	3.14	20.66	x
BSPh1-0.5		0.92	14.44	0.45	0.39	87.33	12.55	10.96	1.59	x
BSPh1-0.8	BSPh1	1.71	23.92	0.84	0.33	39.69	21.09	8.37	12.72	x
BSPh1-1.3		2.55	31.92	1.25	0.40	31.84	28.49	9.07	19.42	x
BSPh2-0.4		0.88	13.99	0.41	0.38	92.01	12.15	11.18	0.97	x
BSPh2-0.8	BSPh2	1.77	24.58	0.83	0.37	44.32	21.69	9.61	12.08	x
BSPh2-1.2		2.58	32.16	1.20	0.40	33.42	28.72	9.60	19.12	x
BSPh3-0.4		1.85	25.41	0.41	0.41	99.51	22.46	22.35	0.11	x
BSPh3-0.8	BSPh3	3.81	41.20	0.84	0.57	67.70	37.33	25.27	12.06	x
BSPh3-1.1		5.71	51.25	1.26	0.57	45.48	47.19	21.46	25.73	x

Polymer: 1g, solvent (THF): 100ml. NN-110: PHPS/xylene solution with 20 wt % of PHPS. Reaction time: 24h, reaction temperature room temperature, under nitrogen gas.

CMS and BS, which were not hydrolyzed, were assumed as S.

Synthesis of nanocomposites

To prepare organic/silica nanocomposites, the block and random copolymers were blended with perhydropolysilazane (PHPS) in THF. The conditions and results are listed in Table IV. The first term and second number of the code indicate the type of organic polymer and the molar ratio of PHPS to hydroxyl group in the blend solution. All blend solutions were not gelated after 24 h from blending. It was previously found that the graft of PHPS onto the hydroxyl group had been completed by 24 h.[12] The high degree of grafting of PHPS onto the polymer is required to control the microphase separation of the nanocomposites. The grafting of PHPS onto the organic polymers was investigated by FTIR. The graft copolymer was separated from the blend solution by precipitation with cyclohexane. Figure 4 shows the FTIR spectra of BSH2 and the graft copolymer formed in BSH2–0.9. For the graft copolymer of BSH2–0.9, the peak of the Si-H bond of PHPS appeared at 2170 cm^{-1}; the grafting of PHPS onto the organic polymers was thus confirmed.

By combination of the peaks of the Si-H bond at 2170 cm^{-1} and of the phenyl group at 1490 cm^{-1}, the grafted amount of PHPS onto the organic polymers was measured. The results are listed in Table IV. The reactivity of the alcoholic hydroxyl group with

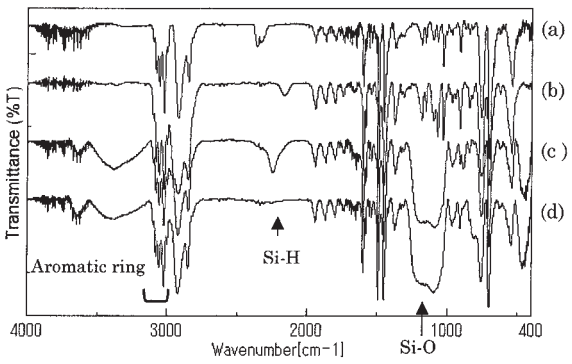

Figure 4 FTIR spectra of organic polymer and the polystyrene/silica composites: (a) BSH2, (b) the graft copolymer in BSH2–0.9, (c) cast film of blend solution of BSH2–0.9, and (d) BSH2–0.9 after calcination.

PHPS is higher than that of the phenolic hydroxyl group. If the reaction were proceeded quantitatively, the grafted amounts of PHPS onto the polymers of the RSH and BSH series should be higher than those of the RSPh and BSPh series, respectively. However, the grafted amounts of PHPS of the RSH series were lower than that of the RSPh series. Additionally, the grafted amounts of PHPS to the hydroxyl group, $[PHPS]_{graft}/[OH]$, of the RSH and BSH series was drastically decreased by increasing the feed amount of PHPS to the hydroxyl group, instead of the fact that the $[PHPS]_{graft}/[OH]$ values of the RSPh and BSPh series were close to 1. The degree of grafting of PHPS of the BSH series was clearly lower than that of the BSPh series. Thus, not alcoholic but phenolic hydroxyl groups quantitatively reacted with PHPS.

The blend was carried out in THF. The hydroxyl group aggregates in THF. The aggregation of the hydroxyl group in THF will decrease the experimental value of the degree of grafting of PHPS onto the alcoholic hydroxyl group from the theoretical value. The aggregation of the organic polymers was investigated by dynamic light scattering (DLS) measurements. Figure 5 shows the DLS profiles of RSPh3, RSH3, BSH1, and BSPh1 in THF. For random copolymers, the peaks of RSPh3 appeared at smaller diameter than RSH3. The diameters of the minimum aggregates were around 10 nm and 120 nm for RSPh3 and RSH3, respectively. The contents of the hydroxyl groups of RSH3, 13.8%, and RSPh3, 10.1%, were close. The size of the aggregates corresponds to interaction between the hydroxyl groups in THF. The hydrogen bonding between alcoholic hydroxyl groups is stronger than that between phenolic hydroxyl groups in THF, since the group molar attraction constants of the alcoholic hydroxyl group and the phenolic hydroxyl group are 225.84 and 170.99 $cal^{1/2}/mL^{1/2}$mole, respectively.[23] The hydroxyl groups of RSH3 and RSPh3

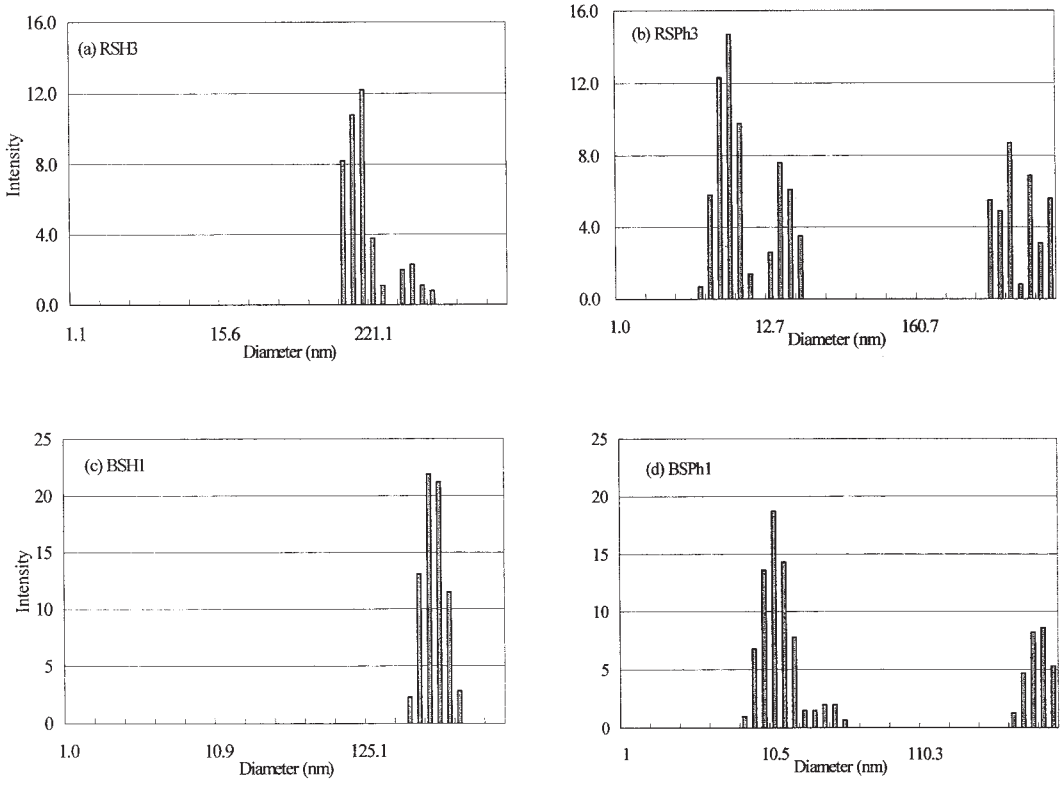

Figure 5 DLS profiles of organic polymers in THF at 0.1 wt % of polymer concentration: (a) RSH3, (b) RSPh3, (c) BSH1, and (d) BSP1h.

were alcoholic and phenolic, respectively. The smaller aggregates around 10 nm of RSPh3 indicates the weak interaction between the phenolic groups in THF. As well as RSH3, the diameters of aggregates of BSH1 were larger than 100 nm. The reacted amount of PHPS onto BSH1 was in a range from 28–9.6 mol %. Therefore, the phenolic hydroxyl group is preferable for the reaction with PHPS in THF. It should be noticed that all composites were prepared by casting the polymer/PHPS blend solution on Teflon substrates. This suggests that the coating film of polymer composites will be prepared by casting the blend solution of polymer and PHPS on typical substrates. The hardness of the composite surface is discussed in a later section.

Microphase separation of nanocomposites

When the phenolic group was used, the grafting of PHPS was improved. Therefore, the better morphology control of nanocomposites was expected not for the RSH series and the BSH series but the RSPh series and the BSPh series. The morphology of microphase separation of the composites was investigated by transmission electron microscopy (TEM). Because of the high electron density of the Si atom in silica, the nanocomposites were not stained for TEM observation. Clear microphase separation was not observed for all nanocomposites with hydroxymethyl styrene units. On the other hand, the nanocomposites prepared with the organic polymers with vinyl phenol units formed clear microphase separation. The composites with RSPh1 and BSPh3 formed especially well-arranged microphase separation. The molar ratios of PHPS reacted with polymer to feed PHPS of the RSPh1 and the BSPh3 series were relatively high. The less silica, which was not grafted onto the polymer, remained in the composites of the RSPh1 and the BSPh3 series. Figure 6 shows the TEM micrographs of the composites with RSPh1. The weight fractions of silica in the composites of RSPh1–1.1 and RSPh1–1.3 are 17.25 and 20.81 wt %. Thus, the expected structures of the microphase separation of RSPh1–1.1 and RSPh1–1.3 are silica spheres in organic matrices. In Figures 6a and 6b, dark spherical domains, which are silica domains, are observed. The average diameters of the silica spheres of RSPh1–1.1 and RSPh1–1.3 were 35 and 43 nm, respectively. The number of silica spheres increased with increasing of the weight fraction of silica. These well agreed to Molau's law.[10]

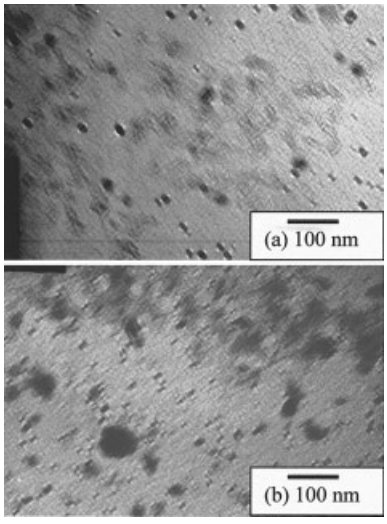

Figure 6 TEM micrographs of the composites: (a) RSPh1–1.1 and (b) RSPh1–1.3.

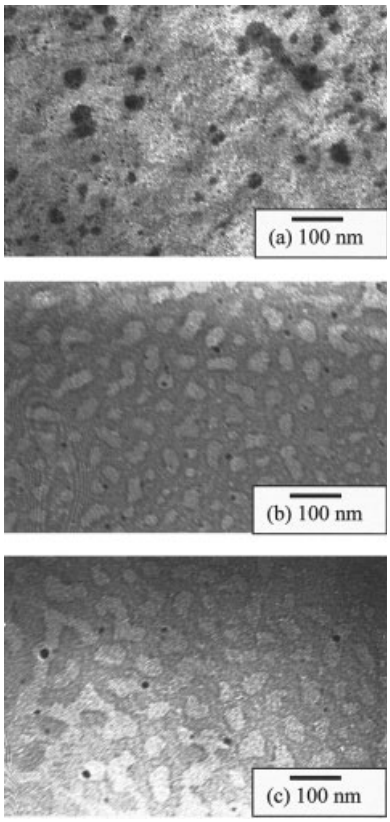

Figure 7 TEM micrographs of the composites: (a) BSPh3–0.4, (b) BSPh3–0.8, and (c) BSPh3–1.1.

Figure 7 shows TEM micrographs of the composites with BSPh3. The weight fractions of silica of the BSPh3 series were from 22.46 to 47.19 wt %. Thus, the change of silica domain structure from spherical to lamella was expected. The structures of BSPh3–0.8 and 1.1 were irregular lamella structures. As well as the PMMA-*block*-P(MMA-*co*-HEMA) and P(MMA-*co*-HEMA), the microphase separation of the nanocomposites was better controlled with P(S-*co*-VPh)-*block*-PS than with P(S-*co*-VPh). The thickness of the PS lamellae, white lamellae, was 35 nm for both BSPh3–0.8 and BSPh3–1.1. The degree of polymerization and number-average molecular weight of the PS sequence of BSPh-3 were 948 and 9.86×10^4, respectively. The lamella thickness of PS calculated from Helfand's equation[24] was 37 nm. The calculated and observed

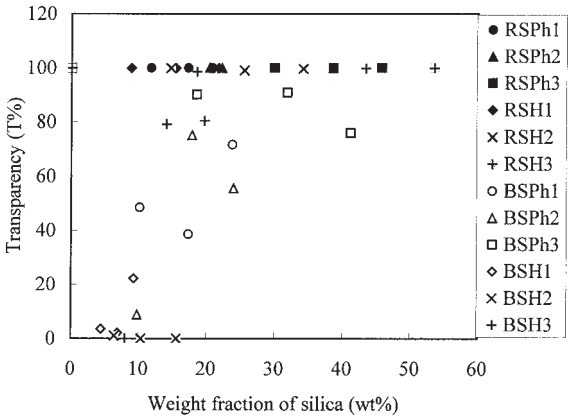

Figure 8 Transmittance of the composite films at 600 nm.

lamella thickness agreed well. Thus, the microphase separation of PS/silica nanocomposites was controlled by varying the weight fraction of silica when block copolymers with vinyl phenol units were used.

Transparency of the composites

Next, the transmittance of the composites was investigated by UV measurements. For a coating material, transparency is one of the important properties. In this work, the transparency of the self-standing film of the composites and coat film of the composites on the glass were estimated. First, the transparency of the self-standing film of the composites at 600 nm is shown in Figure 8. The film thickness was corrected to 1 mm. The composites prepared with random copolymers were highly transparent as well as the polymer films without silica. The transparency of the composites with random copolymers was independent of the content of hydroxyl group, type of hydroxyl group, and silica content. On the other hand, transparency of the composites with block copolymers was strongly dependent on content of the hydroxyl group, type of hydroxyl group, and silica content. The segregation of the PS sequence of the block copolymers would be too strong to form well-arranged microphase separation in the composites. The random copolymer reacted with PHPS would be dispersed in the PHPS domains, and as a result, the block copolymer formed macrophase separation in the composites. Then, the transparency of the composites of RSPh1 and BSPh3 as coat films on glass was measured, from 340 to 1800 nm (Fig. 9). The average thicknesses of the coat films were 1.1 to 3.2 μm. The peak shapes of composites were very close to the glass; the typical absorption owing to the composites was not observed through the entire spectrum. Therefore, because of good transparency, the composites with RSPh1 and BSPh3 were useful materials for coating.

Hardness measurements by the nanoindentation technique

To measure the hardness of the composites with RSPh1 and BSPh3, load-displacement curves were obtained up to maximum loads from 5000 to 50 μN. First, the hardness of self-standing films was measured. Conditions and results at 200 μN are listed in Table V. Film thickness was in a range from 250 to 22 μm. Thus, the influence of a substrate was neglected. Figure 10a shows load-displacement curves of coat film of BSPh3–0.8 on glass at 200 and 1000 μN. Deferent indentations for BSPh3–0.8 performed at different peak loads showed the same variation in the slope of the loading curve. Thus, the consistency of the results was confirmed. Figure 10b shows load-displacement curves at 200 μN maximum loaded obtained for the self-standing films of BSPh3 and their composites. It is clear that the indentation depth after decrease of load from 200 μN to zero was decreased for the composites. The maximum penetration depths obtained lie in the range of 1200–50 nm.

From analysis of a set of curves with different maximum load, the evolution of the hardness values and modulus with the maximum penetration depth of the indenter was estimated. Figure 11 shows hardness of

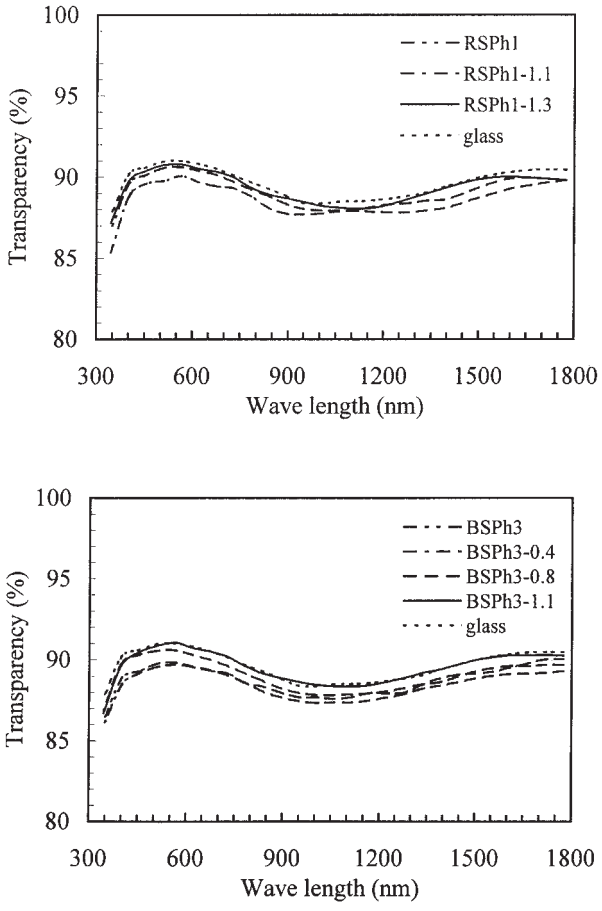

Figure 9 Transmittance of the glass coated with the composites.

TABLE V
Results of Nano-indentation of Organic Polymers and Their Composites

Code[a]	[PHPS]/[OH] (mol/mol)	Silica content (wt %)	Film thickness (μm)	Hardness (GPa)	Modulus (GPa)	Penetration depth (nm)
RSPh1	0.0	0.0	33	0.28	5.1	86.13
RSPh1-1.1	1.1	17.2	110	0.4	7.2	63.75
RSPh1-1.3	1.3	20.8	250	0.34	5.5	72.41
BSPh3	0.0	0.0	22	0.25	5.2	90.27
BSPh3-0.4	0.4	22.5	22	0.57	8.8	38.45
BSPh3-0.8	0.8	37.3	120	0.59	8.9	24.82
BSPh3-1.1	1.1	47.2	30	0.66	9.2	29.79
$RSPh1_{coat}$	0.0	0.0	4.5	0.25	7.4	98.16
$RSPh1\text{-}1.1_{coat}$	1.1	17.2	1.0	0.34	13.5	80.2
$RSPh1\text{-}1.3_{coat}$	1.3	20.8	1.9	0.37	10.8	71.29
$BSPh3_{coat}$	0.0	0.0	2.1	0.25	7.1	94.72
$BSPh3\text{-}0.4_{coat}$	0.4	22.5	2.3	0.46	8.9	52.03
$BSPh3\text{-}0.8_{coat}$	0.8	37.3	3.2	0.63	10.8	33.94
$BSPh3\text{-}1.1_{coat}$	1.1	47.2	1.1	0.74	13.8	28.27

[a] Subscript "coat" indicates the composites on glass.

the composites. The hardness of the coat film decreased at low displacement values and then increased with increasing the displacement values. Since the thickness of the coat film was from 1.1 to 3.2 μm, the hardness of the coat film at high load contains the influence of a substrate. According to Wang and coworkers,[25] the mechanical properties of Teflon film became thickness independent when the film was thicker than 500 nm. On the other hand, the hardness values of self-standing films clearly increased with

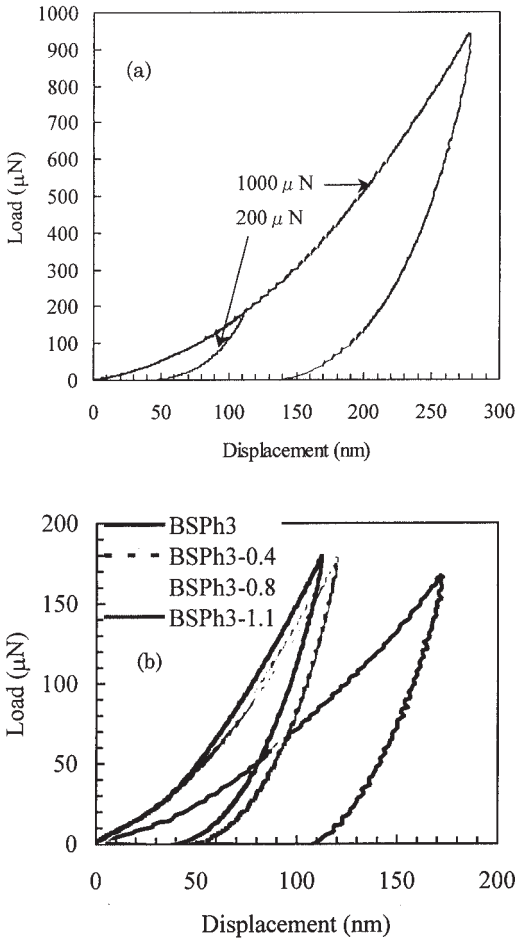

Figure 10 Load-displacement curves of the organic polymers and their composites: (a) BPh3–1.1 on glass, and (b) at 200 μN.

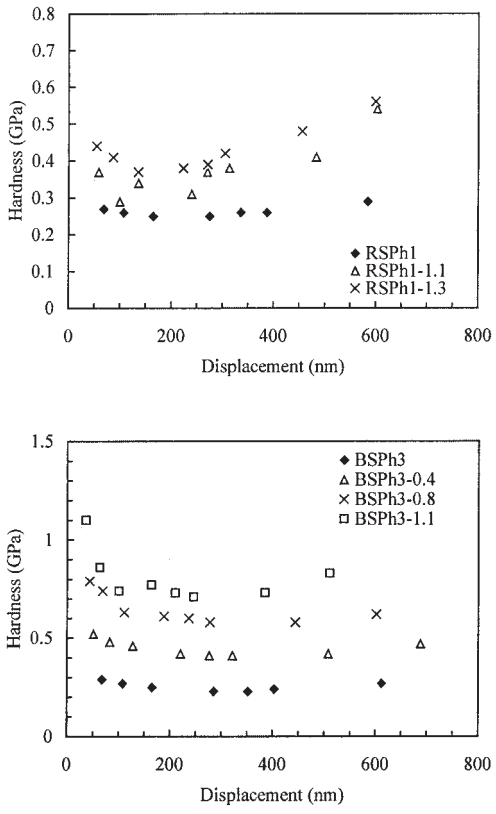

Figure 11 Hardness of the coat films: (a) RSPh1 series, and (b) BSPh3 series.

decreasing the displacement values. Considering the substrate effect, the hardness values at 20% displacement were taken as the real mechanical property in this study. The load was 200 μN. As well as hardness, the moduli at 20% displacement were taken.

The hardness and moduli at 200 μN are listed in Table V. It is clear that the hardness increased with increasing the weight fraction of silica. The difference of surface hardness of the RSPh1 series and the BSPh3 series would not be due to the architecture of the organic polymer but to the silica content in the composites. The range of silica content was 0–20.8 wt % for the RSPh1 series and 0–56.2 wt % for the BSPh3 series. Remarkably, the hardness and modulus of BSP3–1.3 reached 0.66 and 9.2 GPa for the self-standing film, and 0.74 and 13.8 GPa as a coat film on glass, respectively. The surface hardness and modulus of the silica coat prepared by the sol-gel method on polyester was 1.45 and 10.7 GPa, respectively, when the thickness of the silica coat was 128 nm.[22] The silica content of BSPh3–1.3, 56.2 wt %, was clearly lower than the pure silica coat prepared by the sol-gel method. The good hardness of the composites, BSPh3–1.3, would be not only due to the original property of silica prepared with PHPS but also due to the nano-structure formation in the composites. Thus, it was found that nanocomposite of P(S-*co*-VPh)-*block*-PS and silica prepared with PHPS drastically improved the surface hardness. Again, the preparation process of the organic/silica nanocomposites prepared by this work did not require specific treatment after coating on the substrate, except for the heating at 100°C in steam. The surface hardness was drastically improved by coating the nanocomposites. Since the silica content of the coat film was much less than that of the pure silica coat film, the density of the nanocomposite coat film was less than that of the pure silica coat film. Therefore, the organic/silica nanocomposites prepared with PHPS would be useful materials as the light and hard coat film.

CONCLUSIONS

Polystyrene-silica nanocomposites were synthesized by casting the blend solution of perhydropolysilazane (PHPS) and polystyrene with hydroxyl groups. When the copolymers of styrene and vinyl phenol were blended with PHPS, the degree of grafting of PHPS onto the hydroxyl group was larger than that with the copolymers of styrene and hydroxymethyl styrene. From DLS measurements, it was found that the less aggregation of vinyl phenol in the solvent than in hydroxymethyl styrene accelerated the degree of grafting. Clear microphase separation was observed for the composites with poly(hydroxymethyl styrene)-*block*-polystyrene when the degree of grafting was close to 100%. Most of the composites were highly transparent, and the hardness of the composites measured by nano-indentation reached 0.55 Gpa by increasing the silica content in the composites.

References

1. Judeinstein, P.; Sanchez, C. J Mater Chem 1996, 6, 511.
2. Novak, B. M. Adv Mater 1993, 5, 422.
3. Ravaine, D.; Seminel, A.; Charbouillot, Y.; Vincens, M. J Non-Cryst Solids 1986, 82, 210.
4. Judeinstein, P.; Titman, J.; Stamm, M.; Schmid, H. Chem Mater 1994, 6, 127.
5. Brik, M. E.; Titman, J. J.; Bayle, J. P.; Judeinstein, P. J Polym Sci Part B: Polym Phys 1996, 34, 2533.
6. Shimid, H.; Poppal, M.; Rousseau, F.; Poinsignon, C.; Armad, M.; Rousseau, J. Y. 2nd Int Sym Polym Electrolytes 1989, 325.
7. Hsiue, G. H.; Kuo, W. J.; Huang, Y. P.; Jeng, R. J. Polymer 2000, 41, 2813.
8. Chujo, Y. Curr Opin Solid State Mater Eng 1996, 1, 806.
9. Brink, C. J.; Scherer, G. W. Sol-Gel Science: The Physics and Chemistry of Sol-Gel Processing; Academic Press: San Diego, 1990.
10. Molau, G. E. In Colloid and Morphological Behaviour of Block Copolymers; Molau, G. E., Ed.; Plenum Press: New York, 1971.
11. Meier, D. J. Block Copolymers; Science and Technology; Gordon and Breach Science Publisher: Tokyo, 1983.
12. Saito, R.; Kuwano, K.; Tobe, T. J Macromol Sci Pure Appl Chem 2002, A39, 171.
13. Saito, R.; Mori, Y. J Macromol Sci Pure Appl Chem 2002, A39, 915.
14. Mori, Y.; Saito, R. J Macromol Sci Pure Appl Chem 2003, A40, 671.
15. Mori, Y.; Saito, R. Polymer 2004, 45, 99.
16. Saito, R.; Tobe, T. Polym Adv Technol, 2004, 93, 749.
17. Saito, R.; Tobe, T. J Appl Polym Sci, 2005, 16, 232.
18. Benitez, F.; Martinez, E.; Esteve, J. Thin Solid Films 2000, 377–378, 109.
19. Frings, S.; van Nostrum, C. F.; van der Linde, R.; Meinema, H. A.; Rentrop, C. H. A. J Coat Technol 2000, 72, 83.
20. Soloukhin, V. A.; Posthumus, W.; Brokken-Zijp, J. C. M.; Loos, J.; de With, G. Polymer 2002, 43, 6169.
21. Malzbender, J.; de With, G. J Non-Cryst Solids 2000, 265, 51.
22. Chan, C. M.; Cao, G. Z.; Fong, H.; Sarikaya, M.; Robinson, T.; Nelson, L. J Mater Res 2000, 15, 148.
23. Hoy, K. L. J Paint Technol 1970, 42, 76.
24. Helfand, E.; Wasserman, Z. R. Macromolecules 1976, 9, 879.
25. Wang, J.; Shi, F. G.; Nieh, T. G.; Zhao, B.; Brongo, M. R.; Qu, S.; Rosenmayer, T. Scripta Mater 2000, 42, 687.